ScienSage

Journal of Advanced Scientific Research

Available online through https://sciensage.info

ISSN
0976-9595
Research Article

SYNTHESIS OF SILVER NANOPARTICLES USING LEAF EXTRACT OF *ZINGIBER ZERUMBET* (L.) SMITH AND THEIR ANTIBACTERIAL ACTIVITY STUDIES

M. P. Somashekarappa*, H. P. Bhavan

Department of PG Studies in Chemistry, IDSG College, Chikkamagaluru, Affiliated to Kuvempu University, Karnataka State, India

**Corresponding author: mpsomashekar1@gmail.com*

Received: 20-02-2023; Accepted: 27-03-2023; Published: 30-04-2023

© Creative Commons Attribution-NonCommercial-NoDerivatives 4.0 International License https://doi.org/10.55218/JASR.202314405

ABSTRACT

Silver nanoparticles (AgNPs) were synthesized using the leaf extract of a medicinal plant, *Zingiber zerumbet* (L.) Smith. Characterization of the particles was done by UV-visible spectroscopy, scanning electron microscopy (SEM), transmission electron microscopy (TEM) and powder X-ray diffraction (PXRD) studies. TEM analysis shows the presence of spherical and quasi-spherical shaped particles with the maximum of size distribution curve passing through 24 nm. The selected area x-ray diffraction (SAED) pattern and the diffraction pattern from PXRD spectrum indicate that the silver in their nanoparticles crystallize in to face centred cubic (FCC) structure. Bactericidal effect of the synthesized AgNPs against the spreading of gram-negative bacteria, *Escherichia coli (E. coli)* and gram-positive bacteria, *Staphylococcuus aureus (S. aureus)* were determined. The bactericidal effect was determined in terms of minimum inhibitory concentration (MIC) in nutrient agar media, and the MICs are found to be 13.75 $\times 10^{-5}$ g/mL against *E. coli* and 16.50 $\times 10^{-5}$ g/mL against *S. aureus* bacteria. The antibacterial effect exhibited by these AgNPs against both the bacteria is superior compared to that exhibited by the reference compound, ciprofloxacin selected for the study.

Keywords: *Zingiber zerumbet* (L.) Smith, Antibacterial activity, *Escherichia coli, Mirabilis jalapa*, Silver nanoparticles, *Staphylococcus aureus.*

1. INTRODUCTION

Silver nanoparticles are the most studied among the metal nanoparticles [1]. Size-dependant electronic and optical properties of the silver nanoparticles led them to be extensively useful in enormous industrial applications [2]. Most of the technical applications of the AgNPs are attributable to their size, shape and structure dependant surface plasmon resonance [3]. Various fields of technical applications of the AgNPs includes photocatalysis [4], optical sensors [5], nanosphere lithography [6], optoelectronics [7], solar energy conversion devices [8] and surface-enhanced Raman scattering (SERS) substrates [9]. AgNPs are exclusively known for their antimicrobial effects [10] leading them to be applicable in various biomedical applications [11-13]. Remarkable industrial applications of AgNPs owing to their antimicrobial properties encompasses AgNP embedded polyurethane based antibacterial water filter [14], AgNP impregnated blotting paper based point-to-use antibacterial water filter [15, 16], AgNP embedded activated carbon based antibacterial air filter [17] and AgNP embedded textile fabrics possessing antibacterial properties [18-21]. In addition, reviews on the reports related to the application of AgNPs in theranostics [22] and in anti-cancer therapy [23] have been precedented in literature.

Preparation of AgNPs using various harsh chemical reducing agents such as $NaBH_4$, $LiAlH_4$, $R_4N^+(Et_3BH^-)$ or hydrazine [24], results in unstable AgNP solutions contaminated with reaction by-products like borides, metal borates [25], B_2H_6, $NaNO_3$ etc. Preparation of stable AgNP solutions in case of chemical reduction methods demands use of various stabilizing agents [26], certain polymers, and cationic polynorbornenes [27], making the synthesis and stabilization of AgNPs expensive harmful and multistep one's. Though synthesis of AgNPs using mixed-valence polyoxometallates, polysaccharide, Tollens irradiation and other biological methods are considered as greener approaches [28], the synthesis of AgNPs using extracts of plants, bacteria, fungi and biopolymers are greener and cheaper method

in recent years [29-31]. As the AgNPs synthesized from plant extracts are proved to be more sensitive towards biosensing of fungicide and photocatalytic activity [32], and as they are proved to have broader pharmacological applications in treatment of cancer, malaria, microbial and cardiovascular diseases [33], we found it interesting to explore medicinal plants as green, and eco-friendly sources for synthesis of AgNPs.

The genus Zingiber is the third largest of the family Zingiberaceae, whose members are mostly edible and medical plants comprising a total of 141 species [34]. Plants of this genus have primarily distributed in subtropical and tropical Asia, South America and Africa. Currently, a total of 447 phytochemical constituents have been isolated and identified from this genus, in which volatile oils, diarylheptanoids, gingerols, flavonoids and terpenoids are the major components. Extracts and single compounds from Zingiber plants have been discovered to possess numerous biological functions, such as anti-inflammatory, anticancer, antimicrobial, larvicidal, antioxidant and hypoglycemic activities [33, 34].

Zingiber zerumbet is a perennial herb found in many tropical countries, have been regularly used as food flavouring and appetizer while the rhizomes extracts have been used in traditional medicine to treat various types of ailments such as inflammatory- and pain-mediated diseases, worm infestation and diarrhea [35].

The active chemical constituent in *Z. zerumbet* is Zerumbone and is very much known for its anti-inflammatory, anti-microbial, anti-hypersensitivity, chemopreventive and chemotherapeutic activities [36]. Present paper describes the synthesis of stable AgNPs using the water extract of the leaf sample of *Zingiber zerumbet*, characterization of the paerticles by Uv-visible extinction spectroscopy, powder X-ray diffraction, SEM and TEM analysis, and the study of their antibacterial activities against *E. coli* and *S. aureus* bacteria.

2. MATERIAL AND METHODS

2.1. Material

The nutrient agar media was from Himedia. The chemicals were from Merck, or from S. D. Fine chemicals. Distilled water was used wherever required. Bacteria selected for the study were E. coli and S. aurous. A laboratory centrifuge, R-8C from Remi was used for isolation of particles, for SEM and powder XRD analyses. Systronics UV-visible spectrophotometer 119 was used for recording the UV-visible extinction spectra in the wavelength range of 300 nm to 700 nm. Powder XRD patterns were recorded on a Rigacu Smartlab X-Ray diffractometer and the SEM and EDS were recorded on Ultra 55 scanning electron microscope from GEMINI technology. TEM imaging of the drop coated samples were done on Titan Themis 300kV from FEI.

2.2. Methods

2.2.1. Extraction

Freshly collected leaves of the plant were sliced and crushed in to paste with a little amount of warm distilled water using mortar and pestle. The paste was transferred in to a 250 mL beaker, suspended in 100 mL water, stirred on a magnetic stirrer for about 30 minutes at 45-50°C temperature, cooled to lab temperature and filtered through a pre-weighed piece of qualitative filter paper. The weight of the contents transferred to the extract was calculated by difference in weight method. Qualitative phytochemical analysis of the extract was done following a routine method [37].

2.2.2. Synthesis of silver nanoparticles

A 50 ml of the fresh extract containing approximately 0.04 ± 0.005 g/mL of extracted substances was taken in a round bottomed flask fitted with a pressure equalizing dropping funnel. It was heated to 60°C while stirring and 20 mL of 0.002 M $AgNO_3$ solution was added drop wise. Temperature was maintained at 60 ± 5°C during addition of $AgNO_3$ solution and for further 1 hour's time. Contents were cooled to lab temperature. AgNP solution so obtained was centrifuged for isolation of the material, for powder XRD and SEM analyses. The solid was then dried in vacuum over anhydrous phosphorous pentoxide and powdered.

2.2.3. Antibacterial activity studies

A known volume of the AgNP solution was evaporated on a pre weighed watch glass, dried and weighed to determine the amount of AgNP material in its solution. A suspension of 28 grams of nutrient agar in 1000 mL of distilled water was boiled and autoclaved. 20 mL aliquots of the nutrient agar media were contaminated with various increased concentrations of AgNP solutions and transferred in to sterilized Petri dishes. When the media hardened, surface of the media were applied with stains of selected bacteria using cotton swabs. The growth or spread of bacteria was followed for a period of 12 to 15 hours. The standard reference for analysis of the data was the results of same experiments using ciprofloxacin conducted at same condition.

3. RESULTS AND DISCUSSION

A qualitative phytochemical analysis using routine procedures [37] was applied on the water extract with a phytonureient concentration of ~25 $\times 10^{-3}$ g/mL of the leaf sample of *Zingiber zerumbet* (L.) Smith. The extract has shown the presence of carbohydrates and glycosides, saponins, phytosteroids, and phenolic acids and flavonoids, and this data is consistent with that reported by of earlier researchers [35].

Stability and biocompatibility of the AgNPs is a very important requirement for them to be applicable in biology and medicine [28]. Secondary metabolites in the plant extract such as flavones triterpenoids render the extract with free radical scavenging ability [38], and hence the extract possesses reducing nature. Therefore addition of silver salt in to the reducing medium of extract results in reduction of silver salt in to nanocrystalline metallic silver.

3.1. Synthesis

The concentration of phytonutrients in the extract solution is ~8×10^{-4} g/mL. The procedure adopted for the synthesis of AgNPs using leaf extract of *Zingiber zerumbet* (L.) Smith did not use any stabilizing agent and is highly reproducible. Presence of the phenolic componds and flavonoids in the extract as revealed by phytochemical analysis, which is consistent with earlier reports [35] reduces the Ag^+ in the $AgNO_3$ in to atomic silver [30, 39-41] that further coalesce to form nanosized AgNPs. As soon as particles are formed, the oxidized secondary metabolites of the extract after reduction and other bioactive and functional molecules not involved in reduction forms monomolecular layer on the particles [32, 42]. Surfaces of all the particles in the dispersion medium being coated with same kind of organic layer exhibit the same surface charge and hence get repelled from each other. This makes the title AgNP solutions highly stable.

3.2. Characterization

UV-visible absorption spectrum of the AgNPs synthesized using extract of Zingeber zerumbet is shown in Fig. 1.

Silver nanoparticles are known for their characteristic surface plasmon resonance absorption due to surface electrons in the Uv-visible region of electromagnetic radiation [43, 44]. A change in color of the extract from pale green to reddish brown upon addition of silver nitrate in the reaction condition is indicative of formation of AgNPs and could be confirmed by recording a Uv-visible absorption spectrum in the region of 300-700 nm [45, 46]. Absorption spectrum recorded between 300 nm and 700 nm, for dilute extract results in no peaks but only a baseline with a continuum towards 300 nm edge of radiation (Fig.1: (a)). However formation of AgNPs in the solution is indicated by a relatively wider peak with its λ_{max} at 428 nm (Fig.1: (b)). The bigger full width at half maximum (FWHM) of the absorption peak represents the overlapping of several sharp absorption bands, which qualitatively infers a wider distribution of particle size. The Uv-visible absorption spectral data of the AgNPs synthesized from the *Zingiber zerumbet* (L.) Smith is consistent with that of AgNPs synthesized using hydrazine hydrate and sodium citrate as reducing agents [47]. Intensity of the absorption peak at its λ_{max} did not decrease upon repeated recording of the spectrum for the same AgNP solution, with an interval of one week, and for period of 10 weeks, indicating relatively good stability of the particles in the dispersion medium.

Fig. 2 shows the SEM image of the AgNPs synthesized from the leaf extract of *Zingiber zerumbet* (L.) Smith and isolated by centrifugation at 4000 rpm.

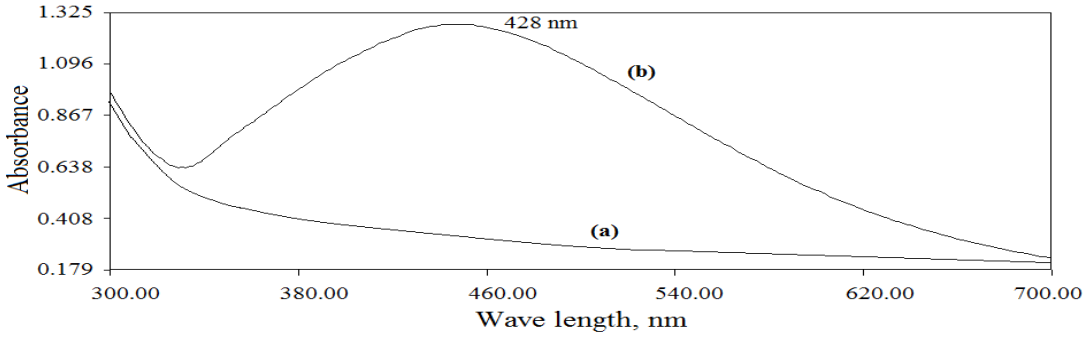

Fig. 1: (a) Uv-visible extinction spectrum of the dilute water extract of leaf sample of *Zingiber zerumbet* (L.) Smith. (b) Uv-visible absorption spectrum of the AgNPs synthesized from the extract of *Zingiber zerumbet* (L.) Smith.

SEM image of the powder sample isolated from the AgNP solution reveals that the spherical particles coalesce to bigger spherical aggregates of 40-120 nm size. Aggregation must have been taken place during centrifugation in order to isolate the material. Profiling of the elements present in the material by point EDS analysis shows 58.62% by weight of silver followed by 16.40 % carbon, 5.42% nitrogen and 19.56% oxygen (inset in Fig. 3: (b)). Presence carbon, nitrogen and oxygen is attributed to the formation of monomolecular layer of the phytonutrient molecules around the particles while stabilizing them. TEM image of the AgNPs drop casted from their solution is shown in Fig. 4.

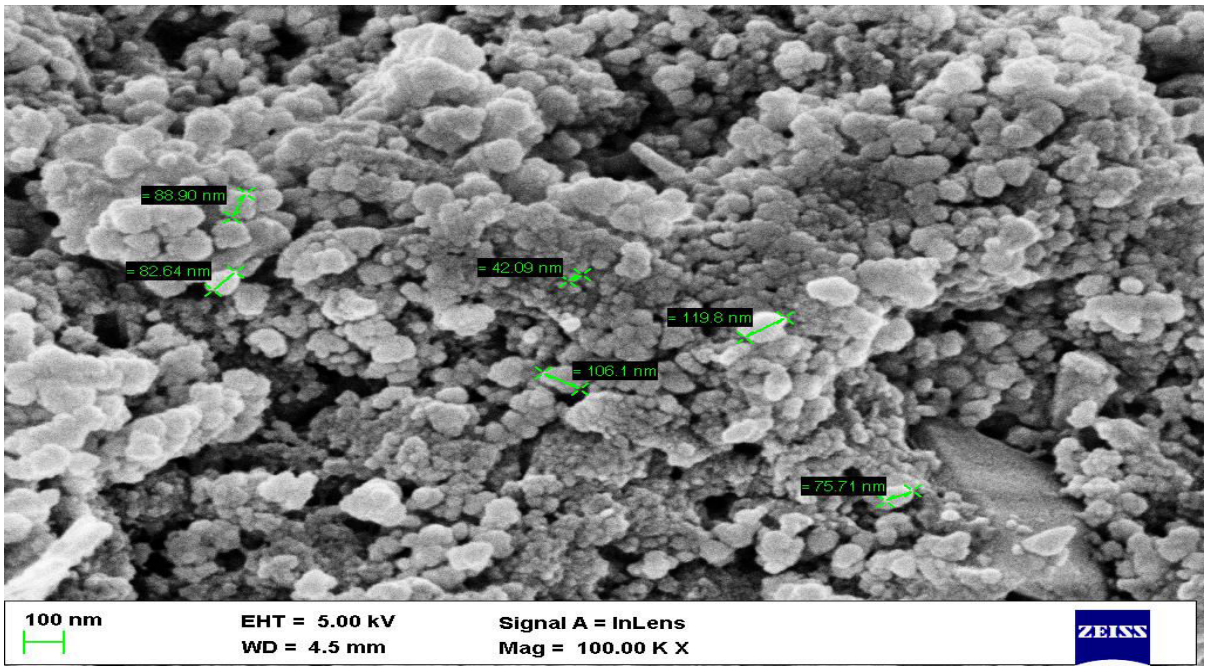

Fig. 2: Scanning electron micrograph of AgNPs synthesized from the aqueous leaf extract of *Zingiber zerumbet* (L.) Smith

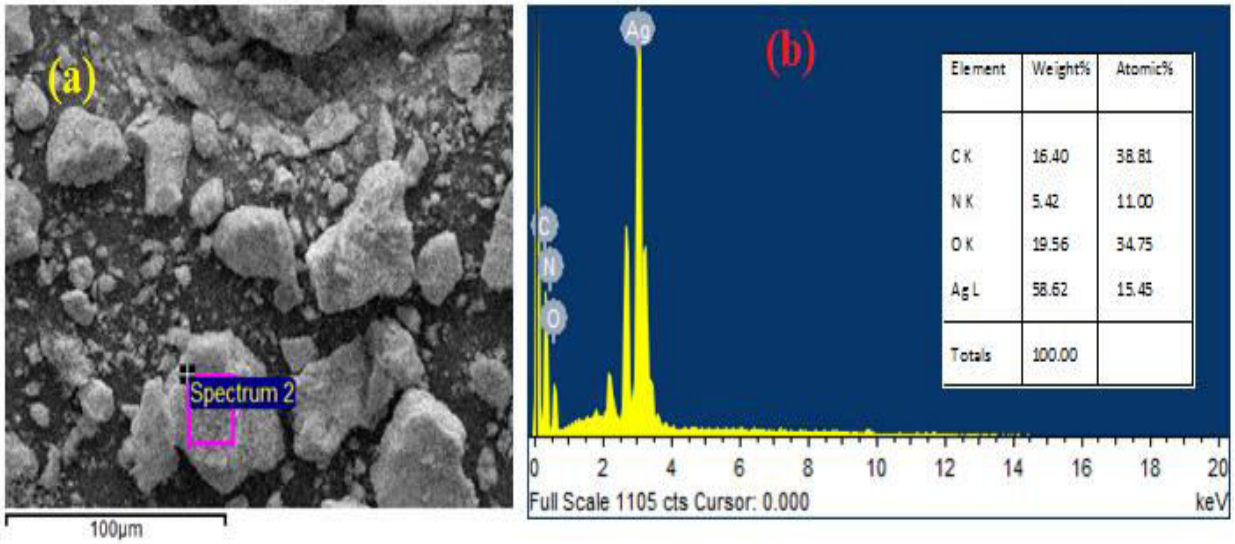

Fig. 3: (a) Micron sized material aggregates upon which the point EDS was recorded and (b) the EDS spectrum of the silver nanoparticles synthesized using the extract of *Zingiber zerumbet* (L.) Smith. Inset in (b) Table showing the elemental percentage of silver, carbon, nitrogen and oxygen in the material.

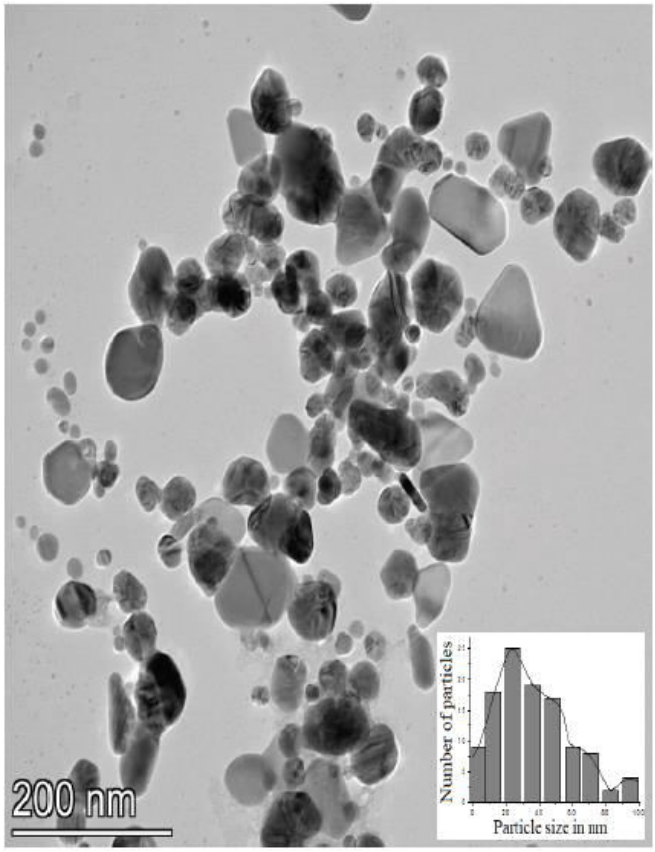

Fig. 4: Transmission electron micrographic image of the AgNPs synthesized from the extract of *Zingiber zerumbet* (L.) Smith. Inset: Histogram showing the particle size distribution worked out upon TEM image.

The shapes of the AgNPs synthesized using leaf extract of title plant are spherical, quasi spherical with a higher percentage of spherical particles. Smaller particles of less than 25 nm appear spherical. TEM results of the present AgNPs agree well with the results of earlier researchers. Selected precedents from earlier workers have mentioned here. AgNPs synthesized form the plant extract of *Terminalia bellirica* [48], and those obtained by extracellular synthesis using Fungus, *Aspergillus niger* are spherical [49]. However, AgNPs synthesized using apiin as reducing agents are quasis pherical in shape [50]. A histogram fit as inset in Fig. 4 represents the size distribution of the particles worked out upon TEM image. It is clear that the particles size distribution is wider and its maximum passes across 24 nm. The qualitative assessment of the wider particle size distribution from the Uv-visible extinction spectrum (Fig.1: (b)) is consistent with TEM analytical data. It is understood upon comparing SEM and TEM images that the bigger aggregates of the size ranging between 42 nm and 120 nm, appeared in SEM image must have been formed during centrifugation and drying in vacuum. When AgNPs coated with organic molecular layer are forced against each other under the influence of centrifugal force, tail part of the monomolecular layer on the particles undergo interdigitation and hence agglomerate the particles in to bigger aggregates. A high resolution TEM image of the single 20 nm sized particle is presented Fig. 5 (a).

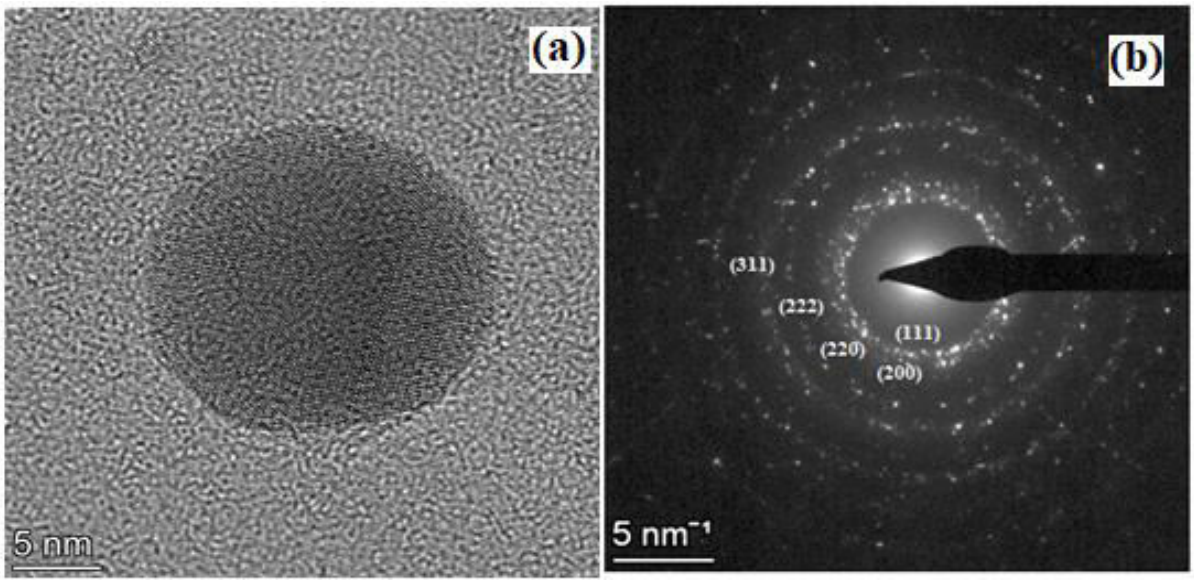

Fig. 5: (a) High resolution TEM image of the single 20 nm sized silver nanoparticle synthesized from the leaf extract of *Zingiber zerumbet* (L.) Smith. (b) SAED pattern on the drop casted layer of AgNP solution.

Selected area electron diffraction (SAED) pattern recorded on a drop casted layer of AgNP solution is shown in Fig. 5(b). Concentric circles with increasing radii and embedded with intermittent bright dots represents the diffractions due to 111, 200, 220, 222 and 311 planes respectively of face cantered cubic (FCC) structure of AgNPs. Thus SAED pattern confirms that Ag^+ in the silver nitrate get reduced to metallic silver by the phytonutrient molecules available in the leaf extract of *Zingiber zerumbet* (L.) Smith, and crystallizes to FCC structure in their nanosized particles [47]. This result is consistent with the FCC structure observed in the silver nanoparticles synthesized by chemical reduction method and by using extract of *Hibiscus rosasinensis* [51].

Crystal structure and average particle size of the title material was further investigated by recording PXRD pattern and the pattern is shown in Fig. 6.

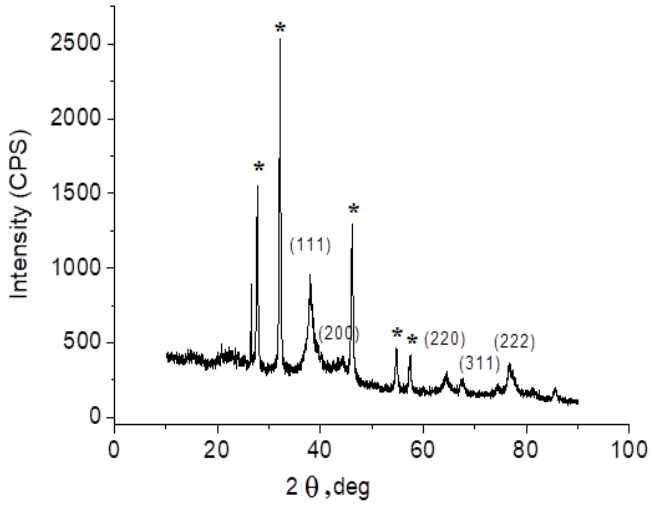

Fig. 6: Powder XRD pattern of AgNPs synthesized from the leaf extract of *Zingiber zerumbet* (L.) Smith.

Positions of the diffractions in 2Θ scale from various cystallographic planes (111), (200), (220), (222) and (311) in the powder XRD pattern reveals the crystallization of silver resulting from phytonutrient mediated reduction of silver nitrate in to FCC structure (JCPDS No. 4-783). Considerably wider FWHM of the characteristic diffraction peaks reveals that the material consists of nanometre sized particles. Average particle size was calculated by substituting the diffraction data corresponding to (111) crystallographic plane in Debye - Scherrer's formula $D = 0.94\ \lambda/\beta \cos\theta$, where D is the average crystalline size, λ is the wavelength of X-ray, β is FWHM and θ is the angle of diffraction. The calculated particle size of the AgNPs synthesized using the leaf extract of *Zingiber zerumbet* (L.) Smith is 17 nm. The average particle size calculated using PXRD method is less than the maximum of the particle size distribution obtained by TEM analysis (inset in Fig. 4). The FCC structure of the AgNPs determined in this work is consistent with that determined for the AgNPs synthesized with the mediation of aqueous extract of *Ocimum Sanctum* and quercetin (a flavonoid from the same plant) [38], root hair extract of *Phoenix dactylifera* [52], extracts of garlic, green tea and turmeric [53], extract of *Sida cordifolia* [54]. The sharp peaks marked by asterisk in PXRD pattern in the Fig. 6 may be ascribed to crystallization of other phytonutrient molecules on the aggregates of the AgNPs.

3.3. Antimicribial activity studies

Antimicrobial activity has been an established characteristic property of the silver nanoparticles [55]. The reports related to the antimicrobial activity studies of silver nanoparticles synthesized by all feasible methods have been elaborately reviewed [56, 57]. In this work we made a relative assessment of the bactericidal ability of AgNPs synthesized using leaf extract of *Zingiber zerumbet* (L.) Smith. Efficiency of the title AgNPs as bactericidal material, against *E. coli* and *S. aureus* bacteria, is established in terms of minimum inhibitory concentration (MIC) of their solid solution in nutrient agar media. The results of this part of the study are presented in Fig. 7 and Fig. 8.

As the concentration of AgNPs in the solidified nutrient agar media increases, growth of the bacteria in both the cases of *E. coli* (Fig. 7) and *S. aureus* (Fig. 8) is diminished. The minimum possible concentration of the AgNPs in the media at and above which the bacterial growth is completely suppressed is considered as minimum inhibitory concentration (MIC). The experimentally determined MIC of the AgNPs synthesized from the leaf extract *Zingiber zerumbet* (L.) Smith are 13.75×10^{-5} g/mL against *E. coli* (Fig. 7) and 16.5×10^{-5} g/mL against *S. aureus* (Fig. 8). in the maintained laboratory conditions. In the same experimental conditions however, the determined MIC of the ciprofloxacin is 20×10^{-5} g/mL against *E. coli* and 24×10^{-5} g/mL against *S. aureus* bacteria. It is established therefore, that the bactericidal efficiency of the AgNPs synthesized using the water extract of the

leaf sample of the *Zingiber zerumbet* (L.) Smith is relatively superior against both the bacteria used in this study, compared to that exhibited by a commercial antibacterial substance ciprofloxacin.

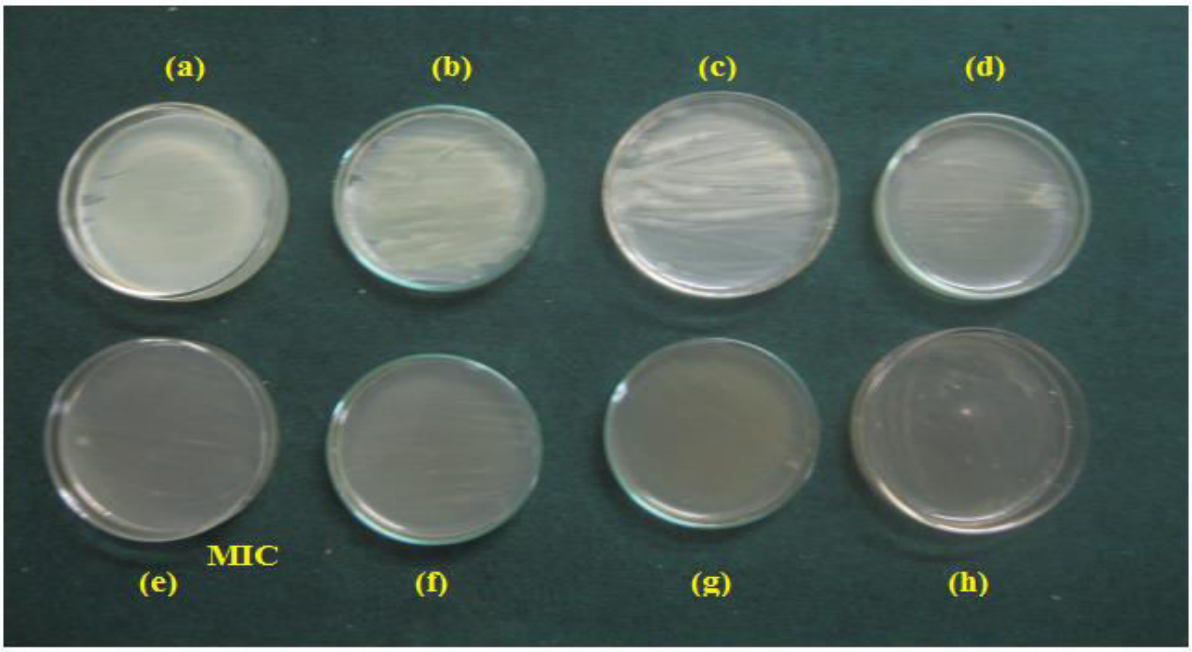

Fig. 7: Growth of the *E. coli* bacteria in 20 ml nutrient agar media contaminated with (a) 0.00 g/ml. (b) 5.50 $\times10^{-5}$ g/mL, (c) 8.25 $\times10^{-5}$ g/mL, (d) 1.10 $\times10^{-4}$ g/mL (e) 1.375 $\times10^{-4}$ g/mL, (f) 1.65 $\times10^{-4}$ g/mL (g) 1.925 $\times10^{-4}$ g/mL, (h) 2.20 $\times10^{-4}$ g/mL of silver nanoparticles prepared from extract of *Zingiber zerumbet* (L.) Smith.

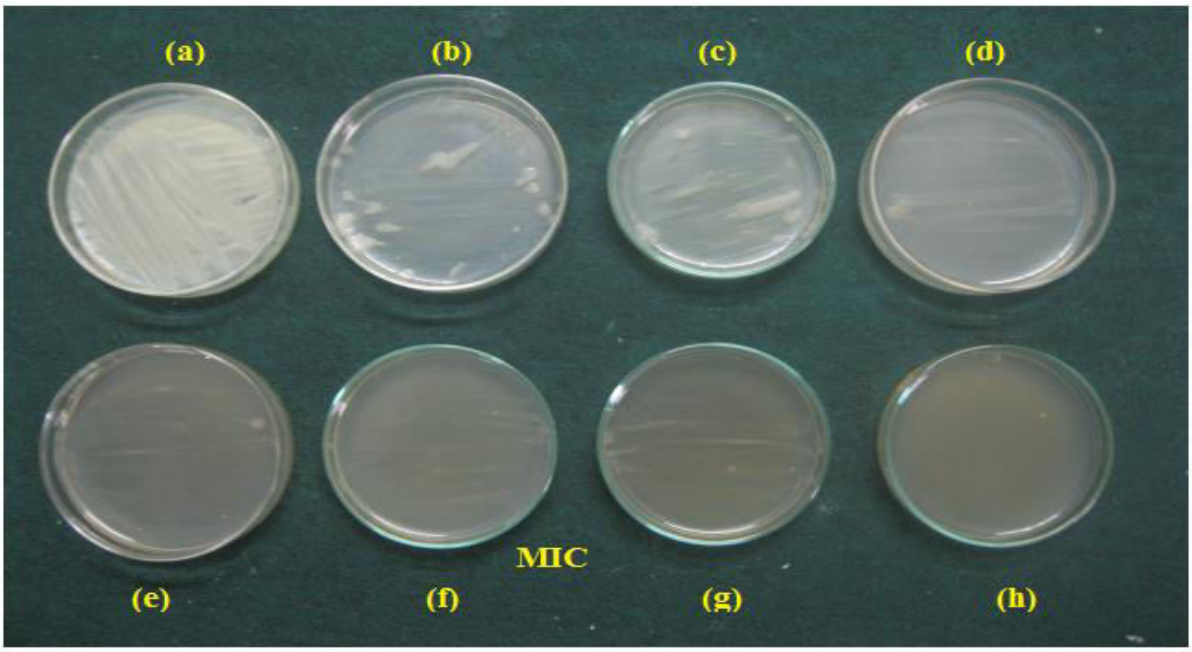

Fig. 8: Growth of the *S. aureus* bacteria in 20 ml nutrient agar media contaminated with (a) 0.00 g/ml. (b) 5.50 $\times10^{-5}$ g/mL, (c) 8.25 $\times10^{-5}$ g/mL, (d) 1.10 $\times10^{-4}$ g/mL (e) 1.375 $\times10^{-4}$ g/mL, (f) 1.65 $\times10^{-4}$ g/mL (g) 1.925 $\times10^{-4}$ g/mL, (h) 2.20 $\times10^{-4}$ g/mL of silver nanoparticles prepared from extract of *Zingiber zerumbet* (L.) Smith.

4. CONCLUSION

The phytochemical molecules analysed to be present in the dilute water extract of the leaf sample of the medicinal plant *Zingiber zerumbet* (L.) Smith such as carbohydrates, glycosides, saponines, phytosteroids, phenolic acids and flavonoids, reduces the silver nitrate resulting in formation of nanosized silver particles followed by capping the particles in order to stabilize them. Thus the AgNPs so obtained are highly stable. The particle size calculated using PXRD pattern is 17 nm whereas maximum of particle size distribution in TEM analysis passes through 25 nm. The diffraction from crystallographic planes in PXRD pattern and the concentric rings in SAED spectrum are in conformity with FCC structure of the particles. The MICs of AgNPs synthesized from the leaf extract of *Zingiber zerumbet* (R.) Smith is 13.75 $\times 10^{-5}$ g/mL against *E. coli* and 16.5 $\times 10^{-5}$ g/mL against *S. aureus* bacteria. The determined bactericidal effect against both the bacterias are relatively better compared to that of the reference compound selected for the study.

5. ACKNOWLEDGEMENTS

Authors thank VGST for awarding a K-FIST level-1 grant which was used to establish basic laboratory facility. Author also thank Micro and Nano characterization facility, Center for nanoscience and engineering, IISc., Bangalore for extending characterization support under INUP programme. Authors also thank Dr. B. Thippeswamy, Department of Microbiology, Kuvempu University for providing bacteria.

Conflict of interest

Authors declare that they have no conflicts of interest.

Source of funding

This research did not receive any specific grant from funding agencies in the public, commercial, or not-for-profit sectors.

6. REFERENCES

1. Beyene HD, Werkneh AA, Bezabh HK, Ambaye TG. *Sustain Mater Technol*, 2017; **13:**18-23.
2. Stark WJ, Stoessel PR, Wohlleben W, Haffner A. *Chem Soc Rev*, 2015; **44**:5793-5905.
3. Amendola V, Bakr OM, Stellacci F. *Plasmonics*, 2010; **5:**85-97.
4. Awazu K, Fujimaki M, Rockstuhl C, Tominaga J, Murakami H, Ohki Y, et al. *J Am Chem Soc*, 2008; **130(5)**:1676-1680.
5. McFarland AD, Van Duyene RP. *Nano Lett*, 2003; **3**:1057-1062.
6. Jensen TR, Malinsky MD, Haynes CL, Van. Duyne RP. *J Phys Chem B*, 2000; **104**:10549-10556.
7. Ko S-J, Choi H, Lee W, Kim T, Lee BR, Jung J-W, et al. *Energ Environ Sci*, 2013; **6:**1949-1955.
8. Morfa AJ, Rowlen KL. *Appl Phys Lett*, 2008; **92**:013504.
9. Li W, Guo Y, Zhang P. *J Phys Chem C*, 2010; **114**:6413-6417.
10. Rai M, Yadav A, Gade A. *Biotechnol Adv*, 2009; **27**:76-83.
11. Wong KKY, Liu X. *Med Chem Commun*, 2010; **1**:125 131.
12. Prabhu S, Poulose EK. *Int Nano Lett*, 2012; **2**:32.
13. Burdusel AC, Gherasim O, Grumezescu AM, Mogoanta L, Ficai A, Andronescu E. *Nanomaterials*, 2018; **8(9)**:681.
14. Jain P, Pradeep T. *Biotechnol Bioeng*, 2005; **90**:59.
15. Dankovick TA, Gray DG. *Environ Sci Technol*, 2011; **45**:1992-1998.
16. Praveena SM, Karuppaiah K, Than LTL. *Cellulose*, 2018; **25**:2647-2658.
17. Yoon KY, Byeon JH, Park CW, Hwang J. *Environ Sci Technol*, 2008; **42**:1251-1255.
18. Ravindra S, Mohan YM, Reddy NN, Raju KM. *Colloids Surf A: Physicochem Eng Asp*, 2010; **367**:31-40.
19. Song J, Kang H, Lee C, Hwang SH, Jang J. *ACS Appl Mater Interfaces*, 2012; **4**: 460-465.
20. Wu M, Ma B, Pan T, Chen S, Sun J. *Adv Functional Mater*, 2016; **26(4)**:569-576.
21. Zhang S, Tang Y, Vlahovic B. *Nanoscale Res Lett*, 2016; **11**: 80.
22. Shaki Devi R, Girigoswami A, Siddarth M, Girigoswami K. *Appl Biochem Biotechnol*, 2022; **194**:4186-4219.
23. Chandrakala V, Aruna V, Angajala G. *Emergent Mater*, 2022; **5:**1593-1615.
24. Schmid G, Chi LF. *Adv Mater*, 1998; **10**:515-526.
25. Glavee GN, Klabunde KJ, Sorensen CM, Hadjapanayis. *Langmuir*, 1992; **8**:771-773.
26. Garcia-Barrasa J, López-de-Luzuriaga JM, Monge M. *Cent Eur J Chem*, 2011; **9**:7-19.
27. Baruah B, Gabriel GJ, Akbashey MJ, Booher ME. *Langmuir*, 2013; **29**:4225- 4234.

28. Sharma VK, Yngard RA, Lin Y. *Adv Colloid and Interface Sci*, 2008; **145**:83-96.
29. Mittal AK, Chisti Y, Banerjee UC. *Biotechnol Adv*, 2013; **31**:346-356.
30. Rajeshkumar S, Bharath LV.*Chem – Biol Interactions*, 2017; **273**:219 -227.
31. Tarannum M, Divya, Gautam YK. *RSC Adv*, 2019; **9**:34926-34948.
32. Alex KV, Pavai PT, Rugmini R, Shiva Prasad M, Kamakshi K, Chandrashekar K. *ACS Omega*, 2020; **5(22)**:13123-13129.
33. Xulu JH, Ndongwe T, Ezealisiji KM, Tembu VJ, Mncwangi NP, Witika BA, et al. *Pharmaceutics*, 2022; **14:**2437.
34. Deng M, Yun X, Ren S, Quing Z, Luo F. *Molecule*s, 2022; **27(9):**2826.
35. Yob NJ, Jofrry SM, Meor Mohd Affridi MMR, The LK, Salleh MZ, Zakira ZA. *Evid Based Complement Alternat Med*, 2011; Article ID 543216.
36. Singh YP, Girisa S, Banik K, Ghosh S, Swathi P, Deka M, et al. *J Funct Foods*, 2019; **53:**248-258.
37. Raaman N, *Phytochemical Techniques*, New India, Publishing Agency. New Delhi, 2006.
38. Jain S, Mehata MS. *Scientific Reports*, 2017; **7:** Article 15867.
39. Mandal D, Kumar Dash S, Das B, Chattopadhyay S, Ghosh T, Das D, et al. *Biomed. Pharmacother*, 2016; **83**:548-558.
40. Priya RS, Geetha D, Ramesh PS. *Ecotoxicol Environ Saf*, 2016; **134**:308-318.
41. Gopinath K, Kumaraguru S, Bhakyaraj K, Mohan S, Venkatesh KS, Esakkirajan M, et al. *Microb Pathog*, 2016; **101**:1-11.
42. Garcia-Barrasa J, López-de-Luzuriaga JM, Monge M. *Cent Eur J Chem*, 2011; **9**:7-19.
43. Taleb A, Petit C, Pileni MP. *J Phys Chem B*, 1998; **102**:2214-2220.
44. Nogin ov MA, Zhu G, Bahoura M, Adegoke J, Small CE, Ritzo BA, et al. *Opt Lett*, 2006; **31(20)**:3022-3024.
45. Paramelle D, Sadovoy A, Gorelik S, Free P, Hobley J, Fernig DH. *Analyst*, 2014; **139(19)**:4855-4861.
46. Desai R, Mankad V, Gupta SK, Jha PK. *Nanosci Nanotechnol Lett*, 2012; **4**:30-34.
47. Guzman MG, Dille J, Godet S. *Int J Chem Biomol Eng*, 2009; **2**:104-111.
48. Anand KKH, Mandal BK. *Spectrochim Acta A Mol Biomol Spectrosc*, 2015; **135:**639-645.
49. Gade AK, Bonde P, Ingle AP, Marcato PD, Duran N, Rai MK. *J Biobased Mater Bioenergy*, 2008; **2(3)**:243-247.
50. Kasturi J, Veerapandian S, Rajendran N. *Colloids and Surfaces B: Biointerfaces*, 2009; **68(1):**55-60.
51. Philip D. *Physica E: Low Dimens Sys. Nanostruct*, 2010; **42:**1417-1424.
52. Oves M, Aslam M, Rauf MA, Qayyum S, Qari HA, Khan MS, et al. *Mater Sci Eng C*, 2018; **89:**429-443.
53. Selvan DA, Mahendran D, Senthil Kumar R, Rahiman AK. *J Photochem Photobiol B: Biol*, 2018; **180:**243-252.
54. Pallela PNVK, Ummey S, Ruddaraju LK, Pammi SVN, Yoon S-G. *Microb Pathog*, 2018; **124:**63-69.
55. Xiu ZM, Zhang QB, Puppala HL, Colvin VL, Alvarez PJJ. *Nano Lett*, 2012; **12(8):**4271-4275.
56. Le Ouay B, Stellacci F. *Nanotoday*, 2015; **10(3):**339 -354.
57. Roy A, Bulut O, Some S, Mandal AK, Yilmaz MD. *RSC Adv*, 2019; **9:**2673-2702.